A Reconfigurable Broadband Dual-Mode Dual-Polarized Antenna for Sectorial/Omnidirectional Mobile Base Stations

Article *in* Progress in Electromagnetics Research · July 2018

DOI: 10.2528/PIER18050206

CITATIONS

READS
128

4 authors, including:

Ahmed Alieldin
University of Liverpool
20 PUBLICATIONS **26** CITATIONS
SEE PROFILE

Yi Huang
University of Liverpool
400 PUBLICATIONS **2,334** CITATIONS
SEE PROFILE

Manoj Stanley
University of Liverpool
27 PUBLICATIONS **57** CITATIONS
SEE PROFILE

Progress In Electromagnetics Research, Vol. 163, 1–13, 2018

A Reconfigurable Broadband Dual-Mode Dual-Polarized Antenna for Sectorial/Omnidirectional Mobile Base Stations

Ahmed Alieldin[1], Yi Huang[1, *], Stephen J. Boyes[2], and Manoj Stanley[1]

Abstract—This paper proposes a new design of reconfigurable three-sector dual-mode dual-polarized antenna for use primarily in mobile communication base stations. The design offers the flexibility to be used as a sectorial (directive) or omnidirectional base station antenna whenever required. The two different radiating modes (omnidirectional and sectorial) depend only on the excitation scenario. The proposed antenna has the advantages of offering broadband, stable radiation pattern and high polarization purity within the desired frequency band, and a simple feeding structure with a very compact size (less than 800 cm^3) and low profile. The achieved fractional bandwidth is 55.3% (1.7–3 GHz). A prototype antenna was constructed and tested with the two modes of operation. Results demonstrate the principle of the design and show how the design may be packaged in a compact size to offer excellent omnidirectional or sectorial performance which makes this new design an ideal candidate for reconfigurable dual-mode mobile base stations.

1. INTRODUCTION

Dual-polarized antennas with a broad bandwidth (BW) have become necessary requirements for cellular mobile communication systems because of the rapid development of communication technologies [1]. Antenna diversity in space and/or polarization has been used to improve the signal-to-noise ratio (SNR) and system performance [2]. Base station antennas should maintain good impedance matching within the entire frequency band of interest, a stable radiation pattern and also a high polarization purity (PP) simultaneously [3]. The PP is defined as the ratio between co- and cross-polarizations in two orthogonal planes (typically $\pm 45°$ for base station antennas). Commonly the used standard specifications for sectorial base station antenna radiation pattern are horizontal half-power beam width (HPBW) of $65 \pm 5°$, PP $\geq$ 20 dB at boresight and PP $\geq$ 10 dB within the HPBW [4]. Many attempts have been made in 2G, 3G, and 4G frequency bands to meet these specifications. In [5] and [6], two antennas have been proposed for such applications, but the BW is insufficient to meet requirements. In [7], despite the achievement of a high PP, the BW (1920–2200 MHz) of the designed antenna limits its usage for mobile systems. In [8], a multiband array design with a compact structure was introduced using an optimal array scheme but the BW was still limited. In [9], the PP was improved by adding parasitic elements at the expense of the antenna size. In [10], a 3D printed cross-dipole structure was employed, but the design showed some drawbacks as it lacks simplicity and ease of fabrication. In [11], the high capacitive structure at the feeding point limited the power handling capability of the design. Furthermore, in [12], although oval-shaped crossed dipoles were used to improve the BW, the PP is not high enough to meet base station antenna requirements. In [12–17] crossed dipoles were widely used as dual-polarized radiators printed on one side of a dielectric substrate with some limitations in size, BW, radiation pattern stability, and PP.

Received 2 May 2018, Accepted 25 June 2018, Scheduled 26 July 2018

* Corresponding author: Yi Huang (Yi.Huang@liverpool.ac.uk).

[1] Department of Electrical Engineering and Electronics, University of Liverpool, Liverpool, L69 3GJ, UK. [2] Defence Science and Technology Laboratory, UK.

For an omnidirectional base station antenna, the antenna should radiate an approximately constant power density in the azimuth [18, 19]. In [20, 21], four dipoles were used with 90° rotating position but the BW was limited. The BW was improved in [22] by adding parasitic elements to two back-to-back dipoles. Dual-polarization in omnidirectional base station antennas has been achieved with a broadband design [23, 24]. In [23], two separate structures were used with two separate feeds (one for the horizontal polarization and the other for the vertical polarization). Later on, in [24], a monopole antenna was used for vertical polarization a while circular loop was used for horizontal polarization. These structures suffer from having large sizes and insufficient BW.

This paper proposes a design of reconfigurable broadband dual-mode dual-polarized three-sector cross dipoles for mobile stations covering the frequency band from 1.7 to 2.7 GHz. The basic idea of the antenna element was introduced by the authors in [25]. As a further development, a novel design of three-sector dual-polarized antenna is introduced here and a detailed discussion of the antenna element operation principles is presented. The three-sector antenna can operate as a sectorial or omnidirectional base station antenna. If the antennas in the three sectors are fed simultaneously with the same signal in phase, a uniform omnidirectional radiation pattern can be obtained. If the antennas in the three sectors are fed independently with different frequency signals, a directive radiation pattern in each sector is achieved. This can offer the mobile operator the desired flexibility in some cases.

The paper is organized as follows: Section 2 describes the antenna element and its working principles; Section 3 discusses the three-sector antenna in the two modes (omnidirectional and sectorial), its principle of operations, results and, its performance. And finally, conclusions are drawn in Section 4.

2. DUAL-POLARIZED ANTENNA ELEMENT

2.1. Antenna Element Design

In this section, a novel broadband dual-polarized antenna element covering 1.7–2.7 GHz is illustrated and applied as the radiating element in the proposed three-sector reconfigurable antenna. Fig. 1 illustrates the geometry of the antenna element. Generally, we can describe the geometry as two orthogonal half-wavelength dipoles, placed on ±45° with respect to Y-axis respectively in order to provide a polarization diversity capability. The dipole radiating elements are printed on the opposite sides of a double-sided Fr-4 substrate with relative permittivity $\varepsilon_r = 4.3$, loss tangent of 0.025 and, thickness $Hd = 1.6$ mm. Each dipole consists of two slotted ellipses linked to a feeding strip and a connector to excite the dipole. The substrate and dipoles are oriented in the YZ plane. The optimized dimensions are determined as follows (in mm): $Uin = 19$, $Uout = 30$, $Vin = 7$, $Vout = 21$, $S = 8$, $W = 3$, $Ld = 52$ and $P = 40$.

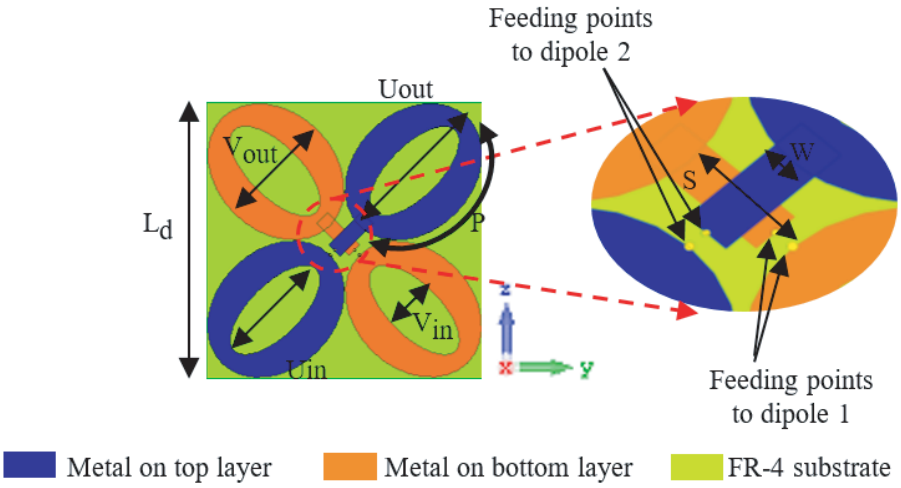

Figure 1. The geometry of the radiating antenna element.

2.2. Principle of Operation

Two reference designs (antenna Ref1 and antenna Ref2) can be employed to understand the working principle of the antenna element as shown in Fig. 2. Initially, the dipole length is set to $0.5\lambda_0$ (antenna Ref1) (where λ_0 is the free space wavelength at the central frequency 2.2 GHz). In this case, the BW observed is narrow. The design is amended to have elliptical-shaped dipoles instead of traditional dipoles as the elliptical radiator dipoles have a wider impedance BW (antenna Ref2) [12]. Initially, the ellipse major and minor axes ($Uout$ and $Vout$) are selected such that the shortest current path length from the feeding point to the end point of the ellipse ($Uout$) equals to $0.25\lambda_{\min}$ while the longest current path length from the feeding point to the end point of the ellipse (P) equals to $0.25\lambda_{\max}$ (where $\lambda_{\min}$ and $\lambda_{\max}$ are the free space wavelength at the highest and lowest frequencies of the desired band at 2.7 and 1.7 GHz respectively and P is half of the ellipse circumference). P is related to the axes length as:

$$P = \pi\sqrt{\frac{\left(\frac{Uout}{2}\right)^2 + \left(\frac{Vout}{2}\right)^2}{2}} = \frac{\lambda_{\max}}{4} \tag{1}$$

It is worth noting that all current path lengths from the feeding point to the ellipse endpoint ranging from the shortest path $Uout$ to the longest path P are equal to a quarter of the wavelengths ranging from $\lambda_{\min}$ to $\lambda_{\max}$ respectively. Thus, the dipole length may be considered as a half wavelength for the all the frequencies within the desired band. In antenna Ref2, the BW observed is wider but is still not

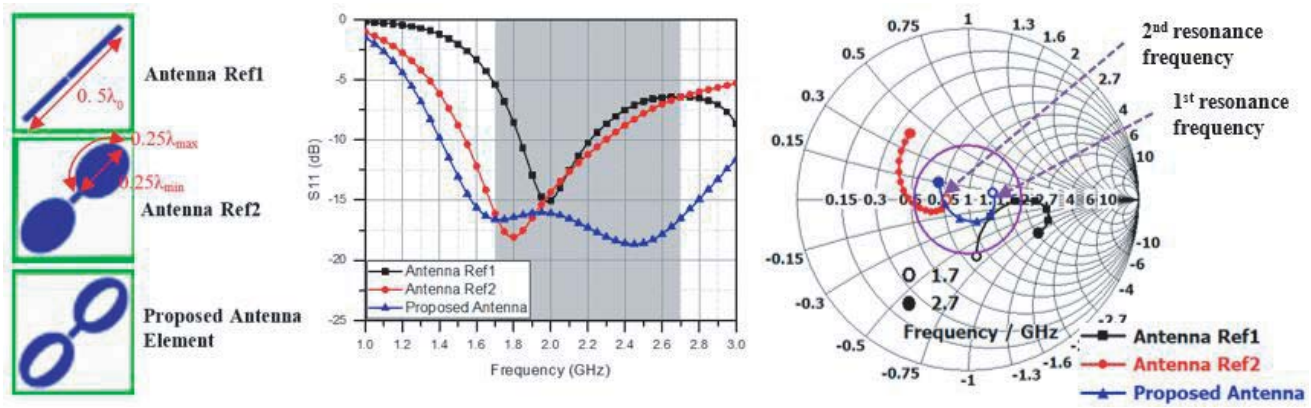

Figure 2. References and the proposed antenna element designs.

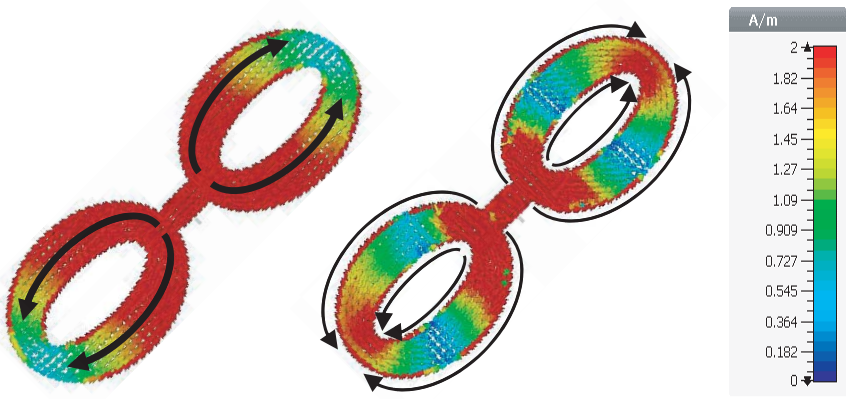

(a) (b)

Figure 3. Dipole current distributions at the resonant frequencies, (a) 1.9 GHz, (b) 2.4 GHz.

satisfactory. This can be improved by further matching the dipole input impedance to the characteristic impedance Z_0 (50 Ω in our case) by cutting an elliptical slot in each arm (proposed antenna element). The major and minor axes of the slot are Uin and Vin respectively which are optimized to achieve minimum reflection coefficient across the desired band. From the Smith chart in Fig. 2, it is evident that the proposed antenna has two resonant frequencies (where the plot intersects the horizontal line of the Smith chart) at 1.9 and 2.4 GHz respectively. Fig. 3 shows the surface current distributions of the radiating dipole at the two resonant frequencies. At the first resonant frequency, the surface current is seen to flow over the dipole surface from the feeding point to the endpoint. At the second resonant, the current flows at the edges of the ellipses and the slots forming another resonator.

3. THREE-SECTOR ANTENNA

In this section, a novel three-sector reconfigurable dual-polarized antenna based on the antenna element presented in Section 2 is designed to operate in one of two different modes; (mode1: omnidirectional

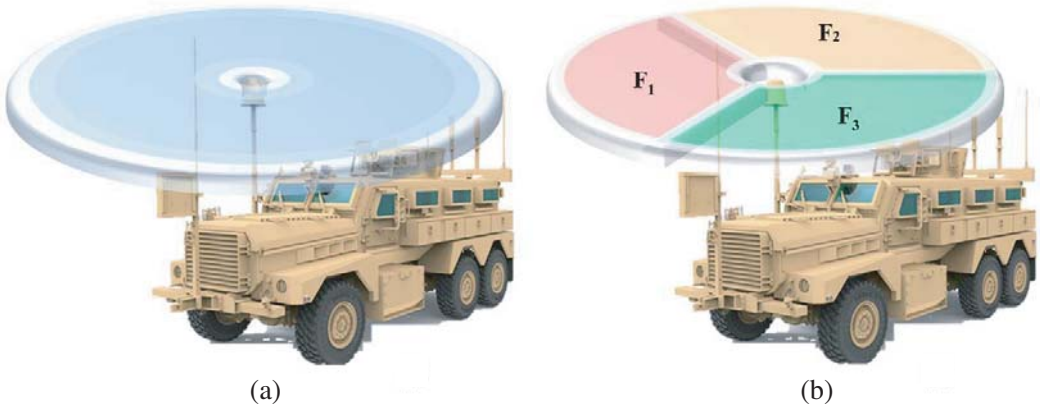

Figure 4. Three-sector antenna modes of operation, (a) omnidirectional mode, (b) sectorial mode (each has a different frequency).

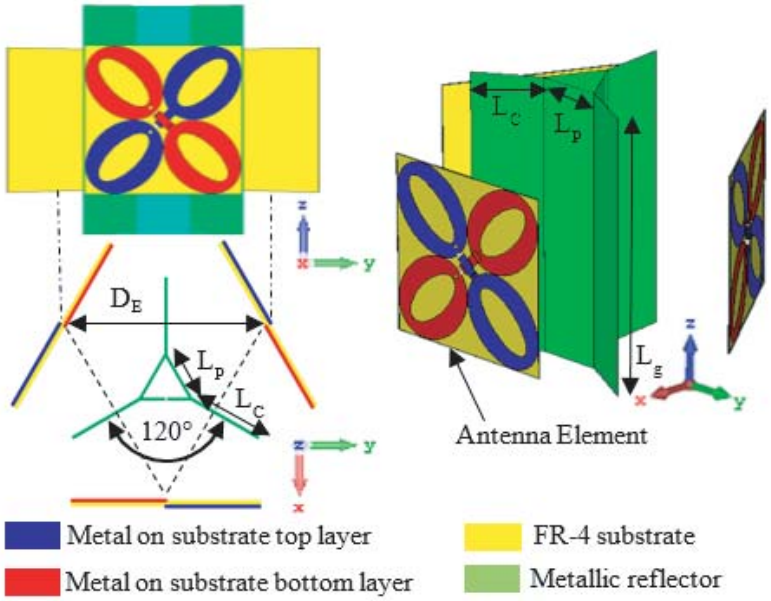

Figure 5. The geometry of the proposed three-sector antenna.

radiation mode and mode 2: sectorial radiation mode). This flexibility in operation offers the advantage that the same single antenna may be used for different applications. The mode of operation for the three-sector antennas (sectorial or omnidirectional) depends only on the excitation mechanism. If the three-sector antennas are fed simultaneously with the same signal (of the same amplitude and phase), an omnidirectional radiation pattern is obtained. However, if the three sectors are fed independently with different frequency signals, a directive radiation pattern in each sector is achieved. This type of varying behaviour can be desirable as a single antenna design could be able to be deployed into different roles if so desired. Fig. 4 shows the two mode-of-operation scenarios using an onboard base station antenna.

The key points of achieving such a design are: (a) optimizing the design of the radiating antenna elements to achieve the optimum impedance matching and port-to-port isolations, (b) constructing a three-sector antenna structure by placing three antenna elements around an equilateral triangular-shaped metallic reflector with a rotating angle of 120° between each pair and as close to each other as possible with accepted degradations in reflection coefficients and isolations, and (c) chamfering the metallic reflector edges L_C with 30° at each side to get suitable radiation patterns in both modes The design is shown in Fig. 5 and detailed dimensions are illustrated in Table 1. The two modes of operation are described in detail as follow.

Table 1. Dimensional parameters of the proposed three-sector antennas.

Dimension	Value (mm)
D_E	60
L_C	24
L_P	10
L_g	80

3.1. Mode 1: Omnidirectional Radiation Mode

The element-to-element separation D_E has a major effect on forming the omnidirectional radiation pattern. For a better understanding of the effect of D_E, let us approximate the equilateral triangular antenna array with a side length of D_E to a circular array with three elements and a radius a as shown in Fig. 6(a) where $a = D_E \tan(30)$. The array factor in XY plane, in this case, equals to [26]

$$AF(\emptyset) = \sum_{m=1}^{3} W_m e^{-j(ka\cos(\emptyset))} = \sum_{m=1}^{3} W_m e^{-j(kD_E \tan(30)\cos(\emptyset))} \tag{2}$$

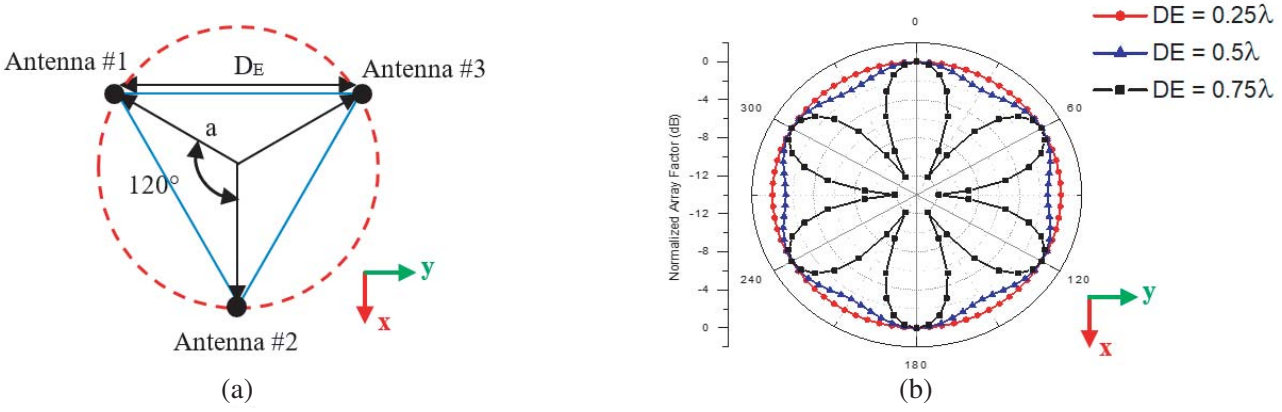

Figure 6. Three-element circular array, (a) structure, (b) array factor.

where Wm is the complex weight of element number m; $k = 2\pi/\lambda$ is the angular wave number; λ is the wavelength; ϕ is the horizontal angle in XY plane. Conventional weights of equal magnitude and phase signals are applied to the six ports. Fig. 6(b) illustrates the array factor as a function of ϕ at different values of D_E in terms of the wavelength. It is clear that the larger D_E is, the higher the difference between peaks and troughs. For a 3 dB-beamwidth of 360° in the horizontal plane, the radiation pattern at any horizontal angle should not exceed 3 dB below the peak value. Fig. 7 illustrates the difference D between peaks and troughs against D_E where

$$D = \max\left(AF\left(\emptyset\right)\right) - \min\left(AF\left(\emptyset\right)\right) \tag{3}$$

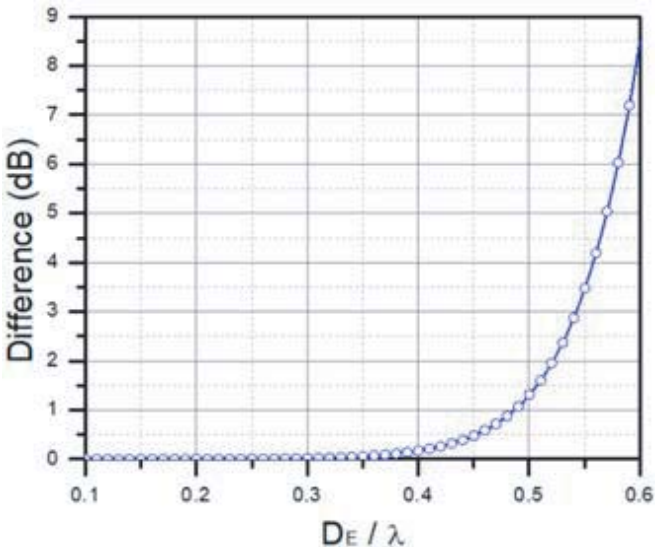

Figure 7. Variation in difference D against D_E.

From Fig. 7, we can see that D_E should not be larger than $0.54\lambda_{\min}$ to ensure the difference $D \leq 3$ dB. Of course the smaller D_E, the more uniform radiation pattern in azimuth. On the other hand, if D_E is too small, the performance will suffer from high reflection coefficients because the radiating antenna elements may become too close to each other and to the common metallic reflector. So, D_E should be chosen carefully as a trade-off between uniform radiation pattern and good reflection coefficients.

The second critical parameter in the proposed three-sector antenna design is the chamfered metallic reflector width L_C. If L_C is small, a uniform radiation pattern in azimuth is easily obtained but on the other hand, the HPBW in sectorial mode would be larger than the desired. If L_C is large, a disturbance in the electric field in azimuth plane may occur and result in a non-uniform radiation pattern. Thus, again the selection of L_C is a trade-off between omnidirectional and sectorial radiation patterns. To validate the design, a prototype of the dual-polarized three-sector antenna element has been manufactured and tested as shown in Fig. 8(a).

Reflection coefficient and isolation between the six ports are measured. For simplicity, Fig. 9 illustrates the reflection coefficient, the worst and the best cases of isolation between any pair of ports. All the other isolation values are in-between the values shown in Fig. 9. There is a good agreement between simulated and measured reflection coefficients of the proposed antenna. A BW of 55.3% (1.7–3 GHz) is achieved for $S_{11} \leq -10$ dB. The isolation between any two ports is better than 18 dB.

To excite the omnidirectional mode, a 6-way equal power divider (typically a three-way power divider for each polarization) is used to feed the antenna ports as shown in Fig. 8(b). The simulated and measured radiation patterns in H-plane (XY plane) and V-plane (XZ plane) for co- and cross-polarizations at frequencies 1.7, 2.2, and 2.7 GHz for the proposed three-sector antenna in omnidirectional mode are plotted in Fig. 10. It is evident that the radiation pattern in the H-plane is approximately uniform with a difference between peaks and troughs ≤ 3 dB and PP better than 20 dB. The HPBWs in the V-plane is $60 \pm 2.5°$.

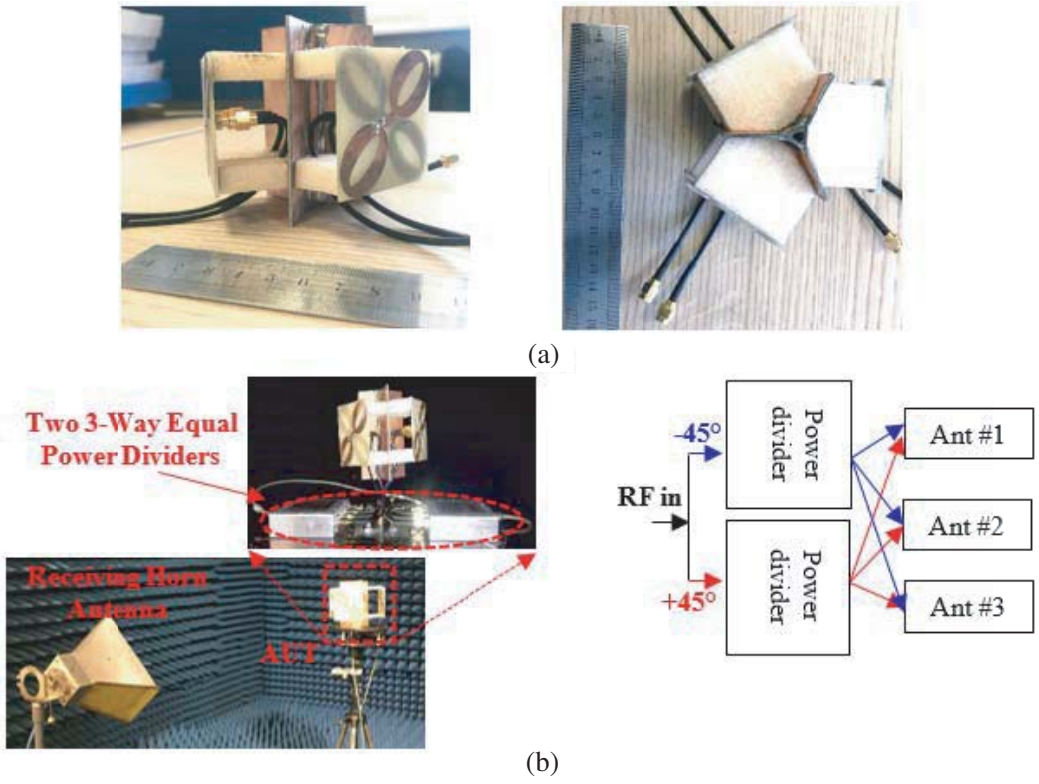

Figure 8. Dual-polarized three-sector antenna, (a) prototype, (b) in omnidirectional mode.

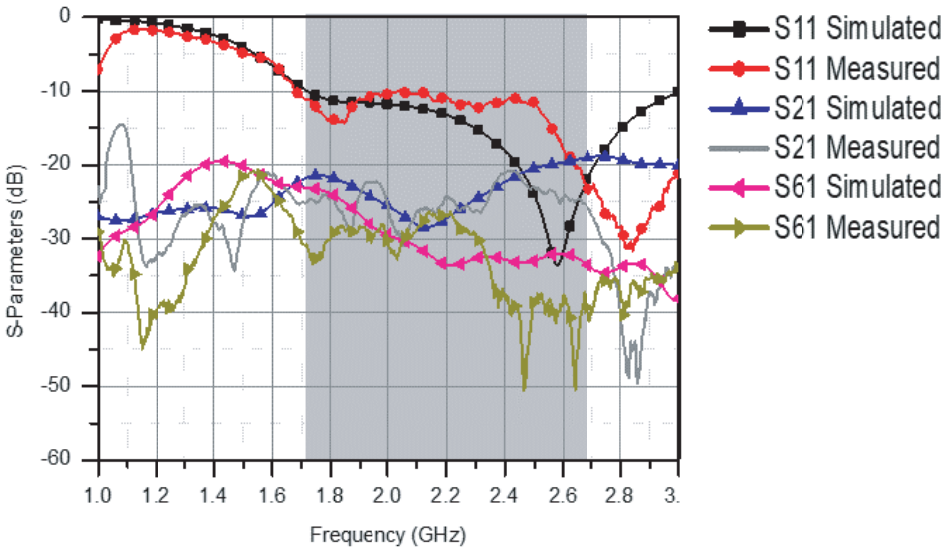

Figure 9. Simulated and measured S-parameter of the three-sector antenna.

Table 2 compares the proposed three-sector antenna in the omnidirectional mode with other reported designs. These designs have a similar frequency band. For a fair comparison, the BWs are chosen with VSWR ≤ 2. It is clear that the proposed design has the widest BW and the smallest size with a relatively high PP. Moreover, it has a dual-polarization of $\pm 45°$ which is typically used in base station antennas rather than the vertical-horizontal (V-H) dual-polarization used in the reference antennas.

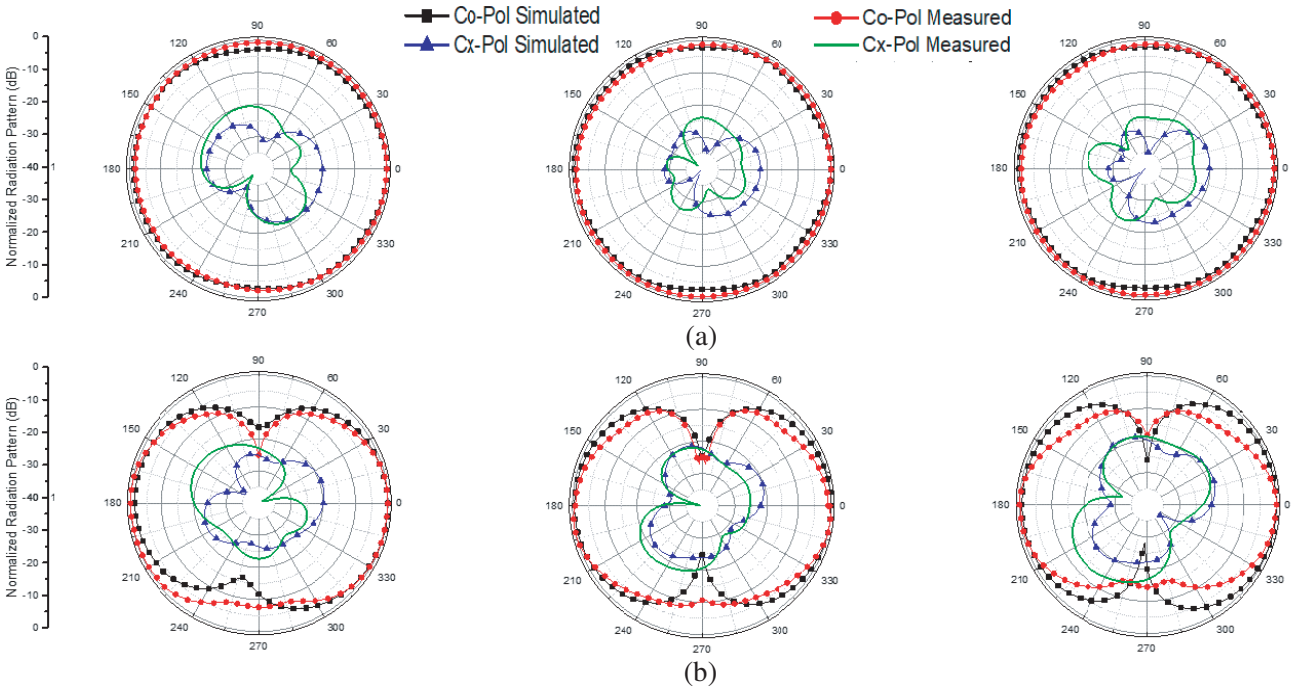

Figure 10. The radiation pattern of the proposed three-sector antenna in omnidirectional mode at (a) H-plane, (b) V-plane.

Table 2. Comparison with reported omnidirectional base station antennas.

Ref.	BW (GHz)	Size (cm^3) ($L \times \pi r^2$)	Polarization	PP (dB)
[20]	1.7–2.2 (25.6%)	814.3	Single (45°)	15
[22]	1.7–3 (55.3%)	1271	Dual (V-H)	22
[23]	1.7–2.7 (45.5%)	942.5	Dual (V-H)	10
This Work	1.7–3 (55.3%)	760	Dual (±45°)	20

The simulated and realized gains are presented in Fig. 11. The proposed antenna has a stable gain of 2.5 ± 0.15 dBi throughout the desired frequency band.

3.2. Mode 2: Sectorial Radiation Mode

In this mode, each pair of orthogonal dipoles in a sector is excited individually by a signal with a different frequency from the other two pairs. Thus, each pair radiates in a specific sector without interfering with the other two pairs in the other sectors. The simulated and measured radiation patterns in H-plane and V-plane for co- and cross-polarizations at frequencies 1.7, 2.2, and 2.7 GHz for the proposed three-sector antenna in sectorial mode are plotted in Fig. 12. The HPBWs for the proposed antenna in the sectorial mode are $68 \pm 3°$ and $60 \pm 2.5°$ in the H-plane and V-plane respectively. As noticed from Fig. 12, the HPBW in the H-plane slightly decreases as the frequency increases, the antenna directivity increases. Fig. 11 shows the proposed antenna radiation efficiency which reaches 98% at 1.7 GHz and slightly decreases as the frequency increases till it reaches 90% at 2.7 GHz due to using a lossy FR-4 substrate. This slight reduction in efficiency compensates the increase in the antenna directivity and hence the realized gain remains almost constant throughout the frequency band. The PP is better than 24 dB at boresight and better than 8 dB within a sector of ±60°. The simulated and measured realized gains of the proposed antenna are plotted in Fig. 11. It is clear that each radiating dipole has a stable gain of 8.5 ± 0.3 dBi across the desired frequency band in the sectorial mode.

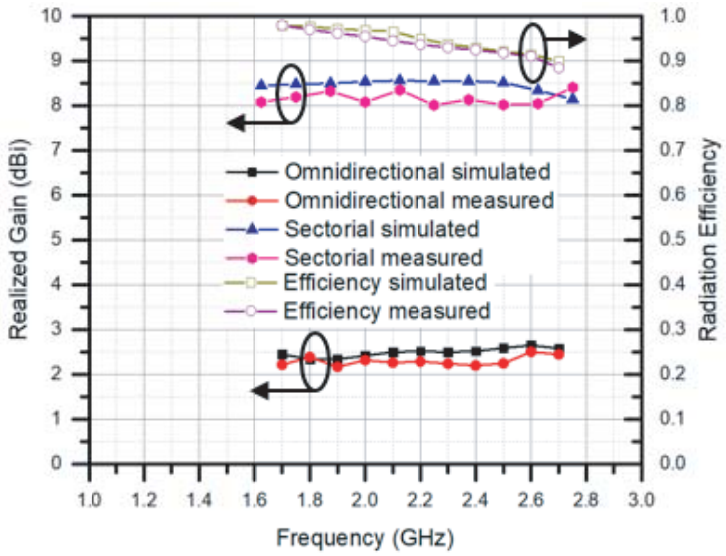

Figure 11. Simulated and measured radiation efficiencies and gains of the proposed antenna in the omnidirectional and sectorial modes.

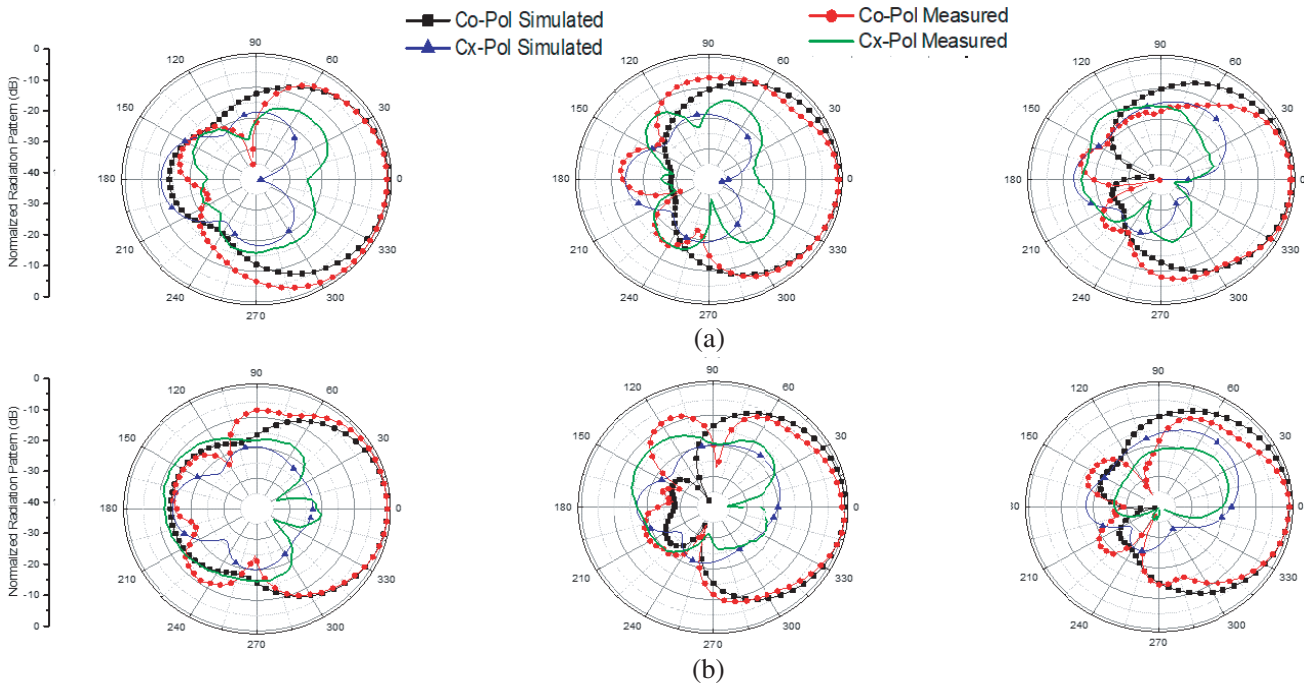

Figure 12. The radiation pattern of the proposed three-sector antenna in sectorial mode at (a) H-plane, (b) V-plane.

Table 3 displays a comparison of antennas in the reference with the proposed sectorial antenna. These antennas have a similar frequency band, working principle and manufacturing process (PCB). The impedance BWs are chosen with VSWR ≤ 2. It can be seen that the proposed antenna has the smallest size and the highest PP at boresight with a relatively high gain and a wide BW as compared to the antennas in [12–17].

Table 3. Comparison with reported directive base station antennas.

Ref	BW	Size (mm^3)	Gain (dBi)	PP (dB)	
				At boresight	Within ±60°
[12]	67%	165 × 165 × 76	8.23	13	5
[13]	55%	150 × 150 × 32	7.8	20	10
[14]	60%	150 × 150 × 31	8.2	20	8
[15]	45%	140 × 140 × 34	8.2	22	8
[16]	70%	150 × 150 × 35	8.8	22	4
[17]	58%	145 × 145 × 35	8.5	18	NA
This Work	55.3%	100 × 80 × 37	8.5	24	8

3.3. Parametric Study

3.3.1. Effect of the Elliptical Slotted Dipoles

A very important parameter in the design is the separation S (see Fig. 1) between the ellipses. As shown in Fig. 13(a), when S increases, the dipole is seen to be more inductive especially at higher frequencies. $S = 8$ mm is found to be the optimum value for VSWR ≤ 2 (the circle in the middle of Smith chart) within the frequency band.

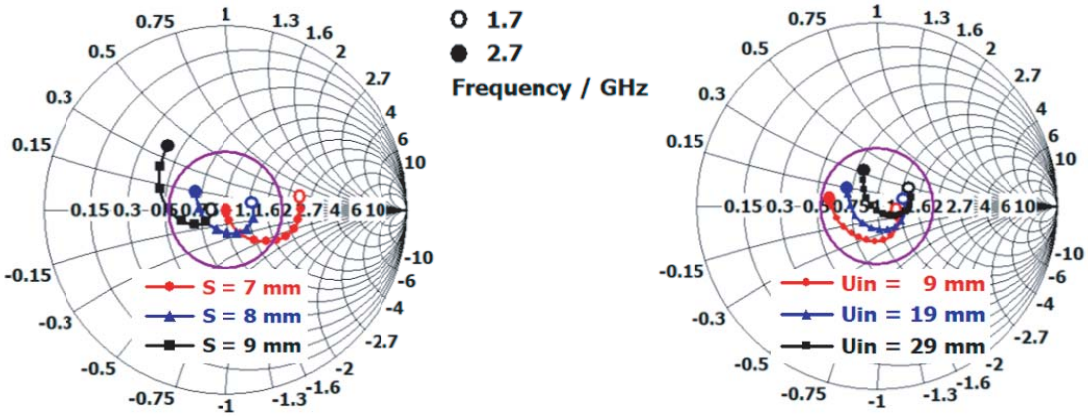

(a) (b)

Figure 13. Effect of (a) S, (b) Uin on the impedance matching.

The second parameter studied is the elliptical slot axis Uin. When this parameter changes, the slot area changes and consequently the impedance matching changes. It is noticeable that the change in Uin affects the shorter current path lengths close to the ellipse major axis ($Uout$) rather than the longer current path lengths close to the ellipse edges (P). Thus, the higher frequencies are more sensitive than the lower frequencies to Uin as shown in Smith chart in Fig. 13(b). Uin is chosen to be 19 mm for optimum impedance matching for VSWR ≤ 2.

3.3.2. Effect of the Triangular-shaped Metallic Reflector

As mentioned in the previous section, D_E has a major effect on forming the uniform radiation pattern in omnidirectional mode. Fig. 14 shows the effect of D_E on both reflection coefficient and omnidirectional radiation pattern at the central frequency 2.2 GHz. It is clear that when $D_E = 50$ mm, although the variation in the radiation pattern is less than 3 dB, the reflection coefficient is not sufficient to cover the

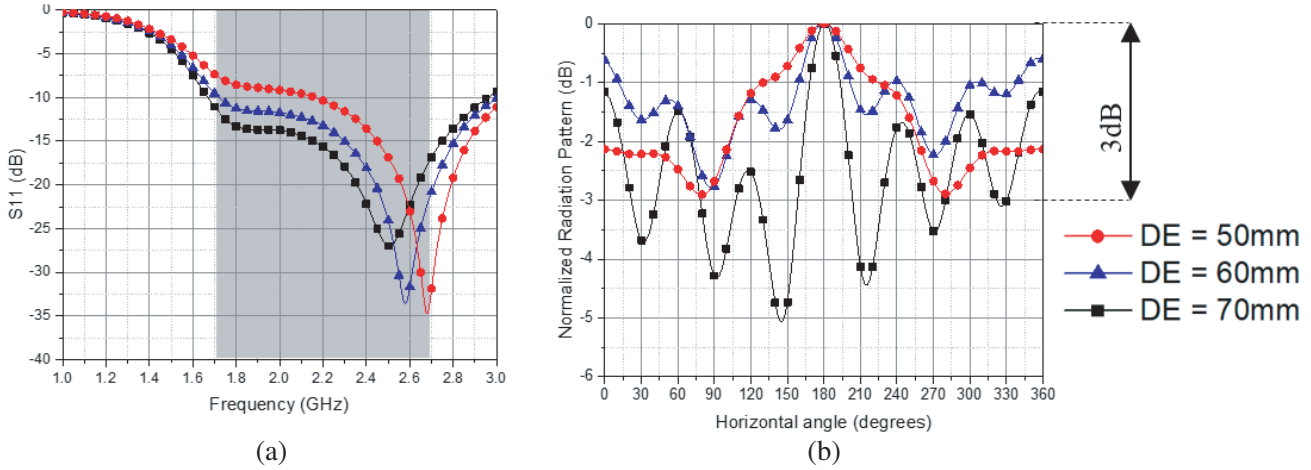

(a) (b)

Figure 14. Effect of D_E on the (a) reflection coefficient, (b) radiation pattern in omnidirectional mode at 2.2 GHz.

desired frequency band because the radiating elements are too close to the metallic reflector. On the other hand, when $D_E = 70$ mm, the reflection coefficient is improved but the variation in the radiation pattern is larger than 3 dB at some horizontal angles in the H-plane. Thus, $D_E = 60$ mm has been found to be the optimum value to achieve a good reflection coefficient and uniform radiation pattern as well.

The second parameter studied is the reflector chamfered edge L_C. Fig. 15 presents the effect of L_C on both the HPBW in sectorial mode and the radiation pattern in omnidirectional mode at the central frequency 2.2 GHz. When $L_C = 20$ mm, the radiation pattern in omnidirectional mode is uniform with spatial variation less than 3 dB between peaks and troughs. But unfortunately, the HPBW in the sectorial mode is too wide to be employed for directive base station antenna (HPBW $\gg 65°$). On the other hand, if $L_C = 28$ mm, the HPBW in sectorial mode is suitable for directive base station antenna but a disturbance in the electric field in omnidirectional mode occurs causing a non-uniform radiation pattern in the H-plane. Thus, L_C was set to 24 mm as an optimum value to achieve suitable HPBW in sectorial mode and a uniform radiation pattern in omnidirectional mode.

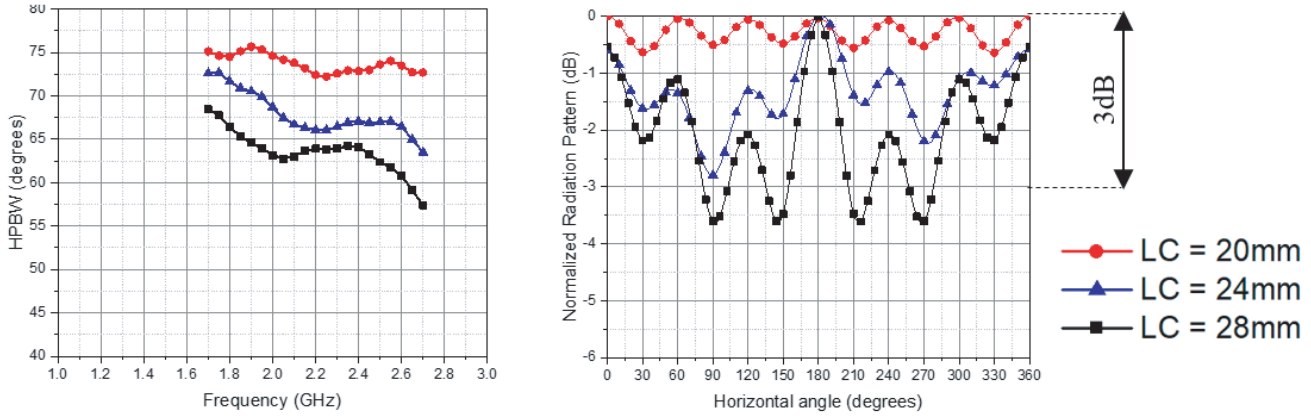

(a) (b)

Figure 15. Effect of L_C on the (a) HPBW in sectorial mode, (b) radiation pattern in omnidirectional mode at 2.2 GHz.

4. CONCLUSIONS

A novel reconfigurable dual-mode three-sector broadband dual-polarized antenna has been designed, optimized, fabricated and measured for mobile communication systems to cover the frequency band from 1.7 to 2.7 GHz. The flexible design performance has the ability to switch between two different radiation modes (omnidirectional or sectorial) only by changing the feeding scenario. The proposed design has been found to have a small size (less than 800 cm^3), high PP, wide BW and, stable radiation pattern. The proposed antenna radiation pattern features meet the base station antenna requirements at both modes in terms of gains, PP and, HPBWs. Thus, a single structure of antenna can be employed to operate at one of two different radiating modes by changing only its excitation mechanism whenever required. The proposed antenna is, therefore, an excellent candidate for reconfigurable dual-mode mobile base stations. The frequency range may be further extended for the 2G/4G applications covering the frequency band from 0.7 to 0.96 GHz or for the new 5G sub-6 GHz bands which is a topic for further investigation.

REFERENCES

1. Wong, K. L., *Compact, and Broadband Microstrip Antennas*, 10, Wiley, Hoboken, NJ, USA, 2002.
2. Mao, X. P. and J. W. Mark, "On polarization diversity in mobile communications," *2006 International Conference on Communication Technology*, 1–4, Guilin, 2006.
3. Chu, Q. X., Y. Luo, and D. L. Wen, "Three principles of designing base-station antennas," *International Symposium on Antennas and Propagation (ISAP)*, 1–3, Hobart, TAS, 2015.
4. Ding, C., H. Sun, R. W. Ziolkowski, and Y. J. Guo, "Simplified tightly-coupled cross-dipole arrangement for base station applications," *IEEE Access*, Vol. 5, 27491–27503, 2017.
5. He, Y., Z. Pan, X. Cheng, Y. He, J. Qiao, and M. M. Tentzeris, "A novel dual-band, dual-polarized, miniaturized, and low-profile base station antenna," *IEEE Transactions on Antennas and Propagation*, Vol. 63, No. 12, 5399–5408, Dec. 2015.
6. Seo, I., et al., "Design of dual polarized antenna for DCS, UMTS, WiBro base stations," *IEEE International Conference on Wireless Information Technology and Systems*, 1–4, HI, 2010.
7. Fhafhiem, N., P. Krachodnok, and R. Wangsan, "Design of a dual polarized resonator antenna for mobile communication system," *International Journal of Electrical, Computer, Energetic and Communication Engineering*, Vol. 8, No. 7, 2014.
8. Jung, Y. and S. Eom, "A compact multiband and dual-polarized mobile base-station antenna using optimal array structure," *International Journal of Antenna and Propagation*, Vol. 2015, 11, 2015.
9. Luo, Y., Q. X. Chu, and D. L. Wen, "A plus/minus 45 degree dual-polarized base-station antenna with enhanced cross-polarization discrimination via addition of four parasitic elements placed in a square contour," *IEEE Transactions on Antennas and Propagation*, Vol. 64, No. 4, 1514–1519, Apr. 2016.
10. Kaddour, A., S. Bories, A. Bellion, and C. Delaveaud, "3D printed compact dual-polarized wideband antenna," *11th European Conference on Antenna and Propagation (EUCAP)*, 3452–3454, 2017.
11. Cui, Y. and R. Li, "Analysis and design of a broadband dual-polarized planar antenna for 2G/3G/4G base station," *11th European Conference on Antenna and Propagation*, 2152–2156, 2017.
12. Huang, D. H. and Q. X. Chu, "Broadband dual-polarized oval-shaped antenna for base-station applications," *2016 IEEE International Symposium on Antennas and Propagation (APSURSI)*, 1859–1860, Fajardo, 2016.
13. Gou, Y., S. Yang, J. Li, and Z. Nie, "A compact dual-polarized printed dipole antenna with high isolation for wideband base station applications," *IEEE Transactions on Antennas and Propagation*, Vol. 62, No. 8, 4392–4395, Aug. 2014.
14. Huang, H., Y. Liu, and S. Gong, "A broadband dual-polarized base station antenna with sturdy construction," *IEEE Antennas and Wireless Propagation Letters*, Vol. 16, 665–668, 2017.

15. Zheng, D. Z. and Q. X. Chu, "A multimode wideband ±45° dual-polarized antenna with embedded loops," *IEEE Antennas and Wireless Propagation Letters*, Vol. 16, 633–636, 2017.
16. Zheng, D. Z. and Q. X. Chu, "A wideband dual-polarized antenna with two independently controllable resonant modes and its array for base-station applications," *IEEE Antennas and Wireless Propagation Letters*, Vol. PP, No. 99, 1–1, 2017.
17. Chu, Q. X., D. L. Wen, and Y. Luo, "A broadband ±45° dual-polarized antenna with Y-shaped feeding lines," *IEEE Transactions on Antennas and Propagation*, Vol. 63, No. 2, 483–490, Feb. 2015.
18. Ando, A., A. Kondo, and S. Kubota, "A study of radio zone length of dual-polarized omnidirectional antennas mounted on rooftop for personal handy-phone system," *IEEE Transactions on Vehicular Technology*, Vol. 57, No. 1, 2–10, Jan. 2008.
19. Li, Y., Z. J. Zhang, J. F. Zheng, and Z. H. Zheng, "Compact azimuthal omnidirectional dual-polarized antenna using highly isolated collocated slots," *IEEE Transactions on Antennas and Propagation*, Vol. 60, No. 9, 4037–4045, 2012.
20. Quan, X., R. Li, Y. Fan, and D. E. Anagnostou, "Analysis and design of a 45° slant-polarized omnidirectional antenna," *IEEE Transactions on Antennas and Propagation*, Vol. 62, No. 1, 86–93, Jan. 2014.
21. Quan, X. and R. Li, "A broadband dual-polarized omnidirectional antenna for base stations," *IEEE Transactions on Antennas and Propagation*, Vol. 61, No. 2, 943–947, Feb. 2013.
22. Yu, Y., J. Xiong, and R. Wang, "A wideband omnidirectional antenna array with low gain variation," *IEEE Antennas and Wireless Propagation Letters*, Vol. 15, 386–389, Dec. 2016.
23. Jolani, F., Y. Yu, and Z. Chen, "A novel broadband omnidirectional dual-polarized MIMO antenna for 4G LTE applications," *2014 IEEE International Wireless Symposium*, 1–4, Xi'an, 2014.
24. Wu, J., S. Yang, Y. Chen, S. Qu, and Z. Nie, "A low profile dual-polarized wideband omnidirectional antenna based on AMC reflector," *IEEE Transactions on Antennas and Propagation*, Vol. 65, No. 1, 368–374, Jan. 2017.
25. Alieldin, A. and Y. Huang, "Design of broadband dual-polarized oval-shaped base station antennas for mobile systems," *2017 IEEE International Symposium on Antennas and Propagation & USNC/URSI National Radio Science Meeting*, 183–184, San Diego, CA, USA, 2017.
26. Balanis, C. A., *Antenna Theory: Analysis and Design*, 3rd edition, Wiley, USA, 2005.